

**Influence of N incorporation on persistent photoconductivity in GaAsN alloys**R. L. Field III,<sup>1,2</sup> Y. Jin,<sup>1,2</sup> H. Cheng,<sup>1</sup> T. Dannecker,<sup>1,2,3</sup> R. M. Jock,<sup>1,2</sup> Y. Q. Wang,<sup>4</sup> C. Kurdak,<sup>1</sup> and R. S. Goldman<sup>1,2,\*</sup><sup>1</sup>*Department of Physics, University of Michigan, Ann Arbor, Michigan 48109-1040, USA*<sup>2</sup>*Department of Materials Science and Engineering, University of Michigan, Ann Arbor, Michigan 48109-2136, USA*<sup>3</sup>*Tyndall National Institute, University College Cork, Cork, Ireland*<sup>4</sup>*Materials Science and Technology Division, Los Alamos National Laboratory, Los Alamos, New Mexico 87545, USA*

(Received 21 December 2011; published 8 April 2013)

We examine the role of N environment on persistent photoconductivity (PPC) in GaAs<sub>1-x</sub>N<sub>x</sub> films. For  $x > 0.006$ , significant PPC is observed at cryogenic temperatures, with the PPC magnitude increasing with increasing  $x$  due to an increase in the density of N-induced levels. Interestingly, rapid thermal annealing suppresses the PPC magnitude and reduces the N interstitial fraction; thus, the N-induced level is likely associated with N interstitials. PPC is attributed to the photogeneration of carriers from N-induced levels to the conduction-band edge, leading to a modified N molecular bond configuration. With the addition of thermal energy, the ground state configuration is restored; the N-induced level is then able to accept carriers and the conductivity decays to its preillumination value.

DOI: [10.1103/PhysRevB.87.155303](https://doi.org/10.1103/PhysRevB.87.155303)

PACS number(s): 72.20.My, 61.72.uj, 71.55.Eq, 73.50.Pz

**I. INTRODUCTION**

In semiconductors, illumination often leads to an increase in the free-carrier density, a phenomenon termed photoconductivity. Following the termination of illumination, typical semiconductors experience carrier relaxation on nanosecond timescales. However, some semiconductors exhibit persistent photoconductivity (PPC), in which an illumination-induced increase in conductivity persists after the termination of illumination,<sup>1-3</sup> with relaxation timescales up to hours or days.<sup>4</sup> PPC is often attributed to the photoexcitation of carriers from a ground state associated with a donor complex to the conduction-band edge (CBE). The subsequent return of carriers to the ground state is hindered by an energy barrier associated with a lattice relaxation needed for the donor complex to accept carriers. In doped Al<sub>y</sub>Ga<sub>1-y</sub>As alloys with  $y > 0.2$ , PPC has been observed and attributed to the photoexcitation of free carriers from a  $DX^-$  donor complex, consisting of threefold coordinated Si<sub>Ga</sub>, to a shallow donor level.<sup>5,6</sup> In the case of InGaAsN alloys, PPC has been attributed to the photoexcitation of free carriers from N-related deep donor<sup>7,8</sup> or acceptor<sup>9</sup> complexes with unspecified atomic structures. Furthermore, in GaAsN alloys, an annealing-induced increase in carrier concentration and a transition from variable range hopping to extended band conduction has been explained by a corresponding decrease in the interstitial N concentration.<sup>10,11</sup> Indeed, the concentration and local atomic environment of solute atoms determine the properties of semiconductor alloys.

In GaAsN alloys, a variety of electronic levels associated with N pairs and/or cluster states—i.e., N-induced levels—have been reported.<sup>12-22</sup> Furthermore, the CBE of GaAsN has been reported to vary with temperature,<sup>23</sup> thus, the positions of the N-induced levels with respect to the CBE may also vary with temperature. It has been reported that the number and positions of the N-induced levels are dependent on [N].<sup>12-16</sup> In the ultradilute [N] regime, single-impurity N levels form a resonant state above the CBE.<sup>24-26</sup> With increasing [N], N pair and cluster states are apparent,<sup>12-18</sup> resulting eventually in the formation of an impurity band.<sup>15,16</sup> Here, we examine the influence of N incorporation on PPC in GaAsN. PPC is

attributed to the photoexcitation of carriers from N-induced levels associated with N interstitials to the CBE, leading to a modification of the N molecular bond configuration. With the addition of thermal energy, the ground state configuration is restored; the N-induced level is then able to accept carriers and the conductivity decays to its preillumination value.

This article is organized as follows. In Sec. II, we describe the methods used for synthesizing and characterizing the GaAs(N) films, including molecular-beam epitaxy (MBE), nuclear reaction analysis (NRA), Rutherford backscattering spectrometry (RBS), and resistivity and Hall measurements. In Sec. III, we present NRA data and both the time and temperature dependence of the GaAsN resistivity and carrier concentration. In addition, a physical model for the origins of the PPC effect is proposed. Finally, a summary is given in Sec. IV.

**II. EXPERIMENTAL METHODS**

GaAs<sub>1-x</sub>N<sub>x</sub> alloy films were grown on (001) semi-insulating GaAs substrates by MBE, using solid Ga, As<sub>2</sub> or As<sub>4</sub>, Si or GaTe (for  $n$ -type doping), and an N<sub>2</sub> rf plasma source. The free-carrier concentrations were 5 to  $13 \times 10^{17} \text{ cm}^{-3}$ , as determined by Hall measurements in GaAs control films. The N composition,  $x$ , in the GaAs<sub>1-x</sub>N<sub>x</sub> layers was adjusted from  $x = 0.0013$  to 0.032 by varying the gas flow rate, monitored by the partial pressure of active N, using a residual gas analyzer, as described elsewhere.<sup>10,11,27,28</sup> For all films, a 250-nm-thick GaAs buffer layer was grown at 580 °C, using a growth and annealing sequence described elsewhere,<sup>29</sup> followed by the growth of a 500-nm GaAs(N):Te or GaAs(N):Si layer in the range 400 to 425 °C.<sup>28</sup> For select films, postgrowth rapid thermal annealing (RTA) was performed from 650 to 780 °C for 60 s in an N<sub>2</sub> atmosphere, with a GaAs proximity cap to prevent As outdiffusion.

The N composition and the interstitial N fraction,  $f_{\text{int}}$ , were determined using NRA and RBS of GaAsN and GaAs films in both [001] nonchanneling and channeling conditions. NRA measurements were performed with the <sup>14</sup>N( $d,\alpha_0$ )<sup>12</sup>C

and  $^{14}\text{N}(d,\alpha_1)^{12}\text{C}$  reactions. A 1.2-MeV deuterium ion beam was incident on the GaAsN films, and the yields of the reaction-emitting particles ( $\alpha_0$  and  $\alpha_1$ ) were then detected by a silicon surface-barrier detector located at  $150^\circ$  with respect to the incident beam direction. A range foil of 12- $\mu\text{m}$ -thick mylar was placed in front of the detector to filter out scattered deuterium particles.

Using both van der Pauw and Hall bar geometries, variable  $T$  resistivity and Hall measurements were performed from 1.6 K to room temperature. For the PPC effect study, each film was illuminated using a light-emitting diode (LED) emitting at  $945 \pm 5$  nm. To achieve thermal equilibrium prior to illumination, the GaAsN films were cooled to and held at the measurement  $T$  for more than 10 min. The films were then continuously illuminated until the resistivity,  $\rho$ , decreased to saturation. After the LED was switched off,  $\rho$  was recorded as a function of time. To ensure that each set of relaxation data was obtained with the same initial conditions, the films were subsequently reheated (without illumination) to at least 200 K for more than 10 min prior to cooling to the next measurement  $T$ .

### III. RESULTS AND DISCUSSION

#### A. PPC magnitude and electron-capture barrier

In Fig. 1, we plot the magnitude of the PPC effect,  $\sigma_{PPC}^N$ , as a function of  $x$ , measured at 77 K for various GaAs $_{1-x}$ N $_x$ :Si films. We define  $\sigma_{PPC}^N$ , the increase in conductivity following the termination of illumination, normalized to the preillumination conductivity, as follows:

$$\sigma_{PPC}^N = \frac{\sigma_s - \sigma_d}{\sigma_d}, \quad (1)$$

where  $\sigma_d$  is the conductivity prior to illumination and  $\sigma_s$  is the sustained conductivity obtained 1600 s following the termination of illumination. The inset to Fig. 1 shows a typical 77-K PPC trace, whereby a GaAs $_{0.985}$ N $_{0.015}$  film, initially in the dark, is illuminated until the conductivity increases

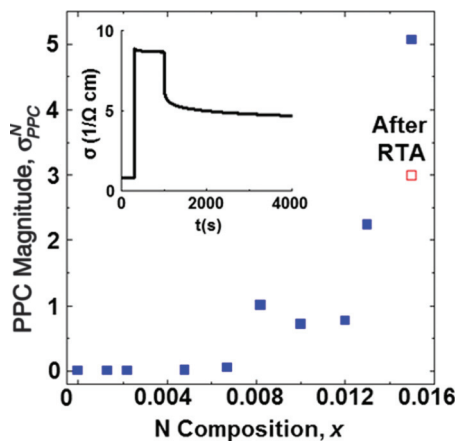


FIG. 1. (Color online) PPC magnitude,  $\sigma_{PPC}^N$ , plotted as a function of N composition,  $x$ , for GaAs $_{1-x}$ N $_x$ :Si films measured at 77 K. Although the PPC effect is negligible for  $x < 0.006$ , it increases with  $x$  for  $x > 0.006$ . The suppression of the PPC magnitude due to 763 °C RTA on a GaAs $_{0.985}$ N $_{0.015}$ :Si film is indicated by the open square. The inset shows a typical PPC trace for a GaAs $_{0.985}$ N $_{0.015}$ :Si film, with an illumination duration from  $t = 300$  to 1000 s.

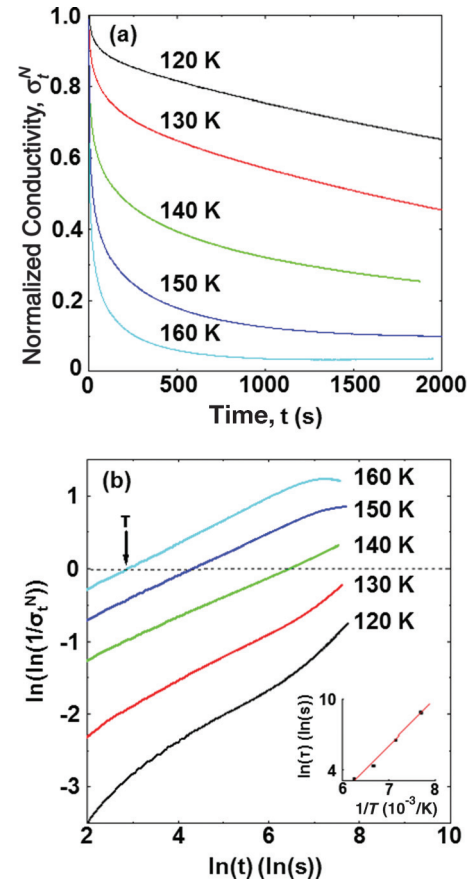


FIG. 2. (Color online) Examples of persistent photoconductivity data and analysis for a GaAs $_{0.987}$ N $_{0.013}$ :Te film. (a) The normalized conductivity,  $\sigma_t^N$ , with  $t = 0$  defined as the instant of illumination termination, plotted as a function of time and measured at various  $T$ . (b) Plot of  $\sigma_t^N$  in the form of a stretched exponential,  $\sigma_t^N \propto \exp[-(t/\tau)^\beta]$ , where the  $x$  intercept at  $y = 0$  is identified as the characteristic decay time,  $\tau$ . The inset shows a plot of  $\ln(\tau)$  vs  $1/T$ , from which the electron-capture energy,  $E_c$ , is determined.

to saturation. Following the termination of illumination, the photocurrent persists for more than 1 h. It is interesting to note that PPC becomes significant for  $x > 0.006$ , due to either an increase in the density of N-induced levels or a change in the relative energy positions of the N-induced level and the CBE, with the N-induced level energy entering the band gap.

To extract the energy barrier hindering the relaxation of photogenerated carriers from the CBE to the ground state of the N-induced level—i.e., the electron-capture barrier,  $E_c$ —the photocurrent was monitored in 10 K increments from 120 to 160 K; in this measurement  $T$  range, the decay timescales were short enough to be measurable. Figure 2(a) shows a typical set of time-dependent normalized photoconductivity data,  $\sigma_t^N$ , for a GaAs $_{0.987}$ N $_{0.013}$ :Te film, with  $t = 0$  defined as the instant of illumination termination. The contribution from photogenerated free carriers, normalized to unity at  $t = 0$ , becomes

$$\sigma_t^N = \frac{\sigma_t - \sigma_d}{\sigma_0 - \sigma_d}, \quad (2)$$

where  $\sigma_0$  is the conductivity at  $t = 0$  and  $\sigma_t$  is the conductivity at time  $t$ .

We consider the photocurrent relaxation process in terms of a stretched-exponential expression:

$$\sigma_t^N \propto \exp \left[ - \left( \frac{t}{\tau} \right)^\beta \right], \quad (3)$$

where  $\tau$  is the characteristic decay time and  $\beta$  is the decay exponent. For this approach, the normalized conductivity is plotted in the form of  $\ln[\ln(1/\sigma_t^N)]$  vs  $\ln(t)$ , as shown in Fig. 2(b), with  $\beta$  ranging from 0.15 to 0.38. At each measurement  $T$ , the available  $x$ -intercepts at  $y = 0$  are identified as  $\tau$ . To minimize extrapolation errors, this analysis only includes data sets that intersect the  $x$  axis in the plot of  $\ln[\ln(1/\sigma_t^N)]$  vs  $\ln(t)$ . The electron-capture barrier is then extracted by plotting the  $T$  dependence of  $\tau$  as

$$\tau = \tau_0 \exp \left( \frac{E_c}{k_B T} \right), \quad (4)$$

where  $k_B$  is the Boltzmann constant and  $\tau_0$  is the high  $T$  limit of  $\tau$ . As shown in the inset of Fig. 2(b), a linear least-squares fit to  $\ln(\tau)$  as a function of  $1/T$  was employed to determine  $E_c$ . Similar analyses reveal an  $E_c$  value of  $280 \pm 20$  meV for  $\text{GaAs}_{1-x}\text{N}_x$  films with  $x$  ranging from 0.0075 to 0.019, apparently independent of  $x$ . We note that the reported variation in CBE over our measurement  $T$  range ( $\sim 10$  meV)<sup>23</sup> is negligible compared with  $E_c$ ; thus, any changes in the alignment of the density of N-induced levels with respect to the CBE is insignificant. The  $E_c$  values for our GaAsN films are comparable to those of GaAsP films ( $120 \pm 30$  meV for Te doping)<sup>30</sup> and AlGaAs films ( $180 \pm 20$  meV for Te doping and  $330 \pm 50$  meV for Si doping)<sup>5,31</sup> but are lower than reported values for unintentionally doped (In)GaAsN alloys (664 meV for  $x = 0.008$ , 570 meV for  $x = 0.013$ , and 349 meV for  $x = 0.018$ ).<sup>7-9</sup> Hence, In may increase the electron-capture barrier in InGaAsN films; the lattice relaxation needed for the N-induced complex to accept carriers might be inhibited by the localization of N at In-rich regions.<sup>32,33</sup>

### B. Activation energy

Typically, the energy to thermally activate carriers from donor states to the CBE is termed  $E_a$ . Therefore, to determine  $E_a$ , we consider the temperature dependence of the carrier concentration for GaAsN films. In addition to N-induced levels, the doped GaAsN:Te (GaAsN:Si) films have a Te-(Si-) induced shallow donor level associated with  $\text{Si}_{\text{Ga}}$  ( $\text{Te}_{\text{As}}$ ). Figure 3 shows  $n$  vs  $1/T$  for various GaAsN films in comparison with that of GaAs:Te. Although  $n$  is independent of measurement  $T$  for GaAs:Te,<sup>34,35</sup> two distinct measurement  $T$  regimes of  $n$  are apparent for the GaAsN films. For low-measurement  $T$ ,  $n$  is independent of  $T$ , presumably due to the low activation energy for the shallow donor levels in GaAsN.<sup>35</sup> For high measurement  $T$ ,  $n$  increases exponentially with increasing measurement  $T$ , suggesting the thermal activation of electrons from N-induced levels to the GaAsN CBE.

To extract  $E_a$ , we assume the coexistence of a shallow donor level and a N-induced level in the context of a two-level system formalism, assuming that the N-induced level follows the CBE<sup>5</sup>

$$\sqrt{n(n - n_s)} \propto \exp \left( - \frac{E_a}{2k_B T} \right), \quad (5)$$

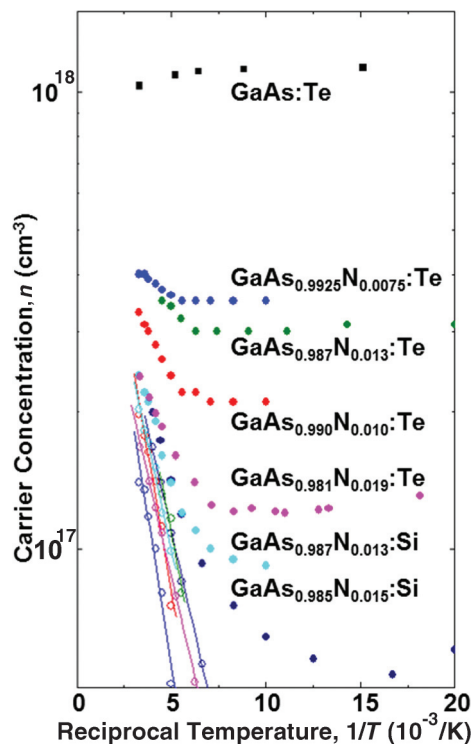


FIG. 3. (Color online) Free-carrier concentration,  $n$ , as a function of  $1/T$  for various GaAsN films in comparison with that of GaAs. For GaAs,  $n$  is  $T$  independent, while for GaAsN, two distinct regimes of  $n$  are apparent: for high measurement  $T$ ,  $n$  increases exponentially with increasing  $T$ ; for low measurement  $T$ ,  $n$  is  $T$  independent. For  $n > n_s$ ,  $\sqrt{n(n - n_s)}$  is also plotted vs  $1/T$  in open circles. A two-level system formalism is then used to extract the energy to activate carriers from donor states to the CBE,  $E_a$ .

where  $n_s$  is the shallow donor concentration, obtained from an analysis of  $n_s$  vs  $T$  data in the low measurement  $T$  regime. In Fig. 3, we plot  $n$  vs  $1/T$  and overlay this with  $\sqrt{n(n - n_s)}$  vs  $1/T$  (in open circles) for  $n > n_s$ .  $E_a$  values are then extracted from the slopes of linear least-squares fits of  $\ln(\sqrt{n(n - n_s)})$  vs  $1/T$  for  $n > n_s$ . For  $\text{GaAs}_{1-x}\text{N}_x$  alloys with  $x$  increasing from 0.0075 to 0.019,  $E_a$  decreases from 105 to 60 meV, as shown in Fig. 4. Hence, as  $x$  increases, the N-induced level presumably remains in the band gap and approaches the CBE. We note that this activation energy is similar to that of Te donors in GaAsP films (70 meV)<sup>30</sup> and also Te and Si donors in AlGaAs films ( $100 \pm 50$  meV)<sup>5,31</sup> but is significantly greater than the activation energy of shallow Te donors (30 meV) and Si donors (4–6 meV) in GaAs.<sup>35,36</sup> In contrast, for  $\text{Al}_y\text{Ga}_{1-y}\text{As}$  alloys, the donor state attributed to PPC enters the band gap for  $y > 0.20$ ,<sup>5</sup> thus, a new PPC mechanism for GaAsN needs to be identified.

Now, we consider the possible composition and temperature dependence of the N-induced level energy. For the composition range  $x = 0.0075$  to 0.019, the observed N composition-dependent decrease in  $E_a$  ( $\sim 45$  meV) is less than the reported decrease in the CBE ( $\sim 130$  meV),<sup>16</sup> implying that the  $x$  dependence of the N-induced level may not follow that of the CBE. For our measurement  $T$  range,  $\sim 150$  to 300 K, the CBE has been reported to be linearly dependent on temperature.<sup>23</sup> Thus, we consider the extreme when the

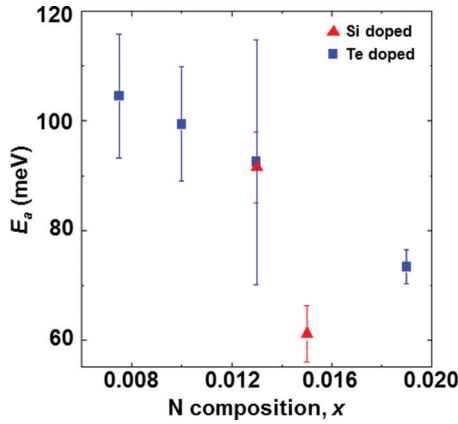


FIG. 4. (Color online) Activation energy from N-induced levels to the conduction-band edge,  $E_a$ , plotted as a function of N composition,  $x$ , for  $\text{GaAs}_{1-x}\text{N}_x$  films. The activation energy decreases with increasing  $x$ , suggesting that the N-induced level energy approaches the CBE as  $x$  increases.

N-induced level remains fixed, while the CBE is linearly dependent on  $T$ . We note that the Arrhenius analysis is insensitive to linear corrections to the energy term; thus, we conclude that  $E_a$  would not be influenced by any  $T$  dependence of the N-induced level energy with respect to the CBE.

**C. Influence of RTA**

To elucidate the origins of the PPC effect in GaAsN, we compare  $E_a$ ,  $\sigma_{PPC}^N$ , and  $f_{int}$  before and after RTA. We note that  $E_a$  remains unchanged after RTA for films of both dopant species (Si vs Te), as discussed in Ref. 11. On the other hand, an RTA-induced reduction of  $\sigma_{PPC}^N$

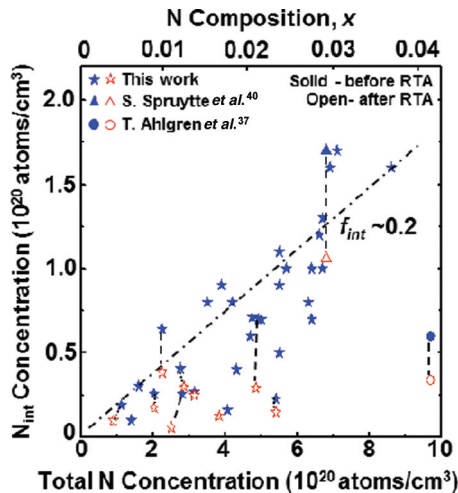


FIG. 5. (Color online) Interstitial N concentration vs total N concentration for  $\text{GaAs}_{1-x}\text{N}_x$  films with various N compositions,  $x$ . Linear interpolation of the interstitial N concentration for as-grown films suggests that approximately 20% of N are incorporated interstitially, as indicated in the plot. Following RTA, the interstitial N concentration decreases to  $\sim 10\%$ , while the total N concentration remains constant to within experimental error. See Ref. 40. See Ref. 37.

for a GaAsN film is shown in Fig. 1. Hence,  $\sigma_{PPC}^N$  is likely influenced by RTA-induced changes in N incorporation mechanisms.

We now consider the influence of RTA on N incorporation mechanisms. In Fig. 5, the measured interstitial [N] is plotted as a function of total [N] for  $\text{GaAs}_{1-x}\text{N}_x$  films with  $x$  ranging from 0.01 to 0.032. The solid blue and hollow red symbols connected with dashed lines represent GaAsN films before and after RTA, respectively. For the as-grown GaAsN films, a linear least-squares fit of the interstitial [N] as a function of total [N] suggests that approximately 20% of N is incorporated interstitially, similar to earlier reports.<sup>27</sup> Following RTA, the total [N] remains constant to within experimental error, while the interstitial [N] is reduced to approximately 10%, possibly due to the diffusion of interstitial N atoms to nearby As vacancies.<sup>37</sup>

**D. PPC mechanism in GaAsN**

In many doped semiconductor alloys, PPC has been observed and attributed to the photoexcitation of free carriers

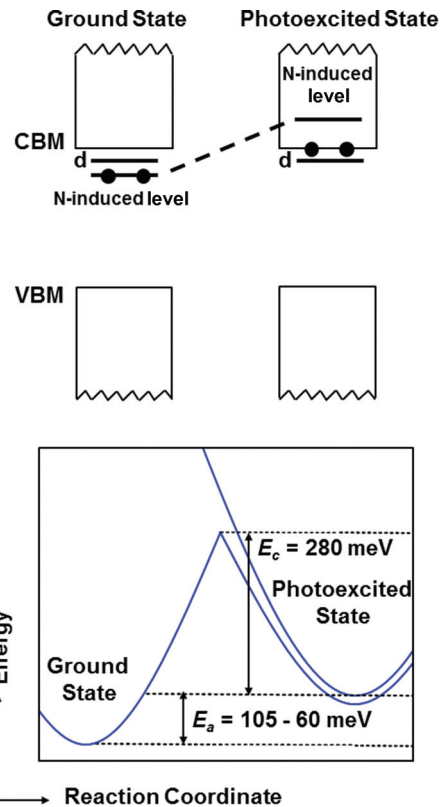


FIG. 6. (Color online) Schematic energy diagram of “ground” (left) and “photoexcited” (right) states GaAsN. Prior to illumination, carriers reside in the ground state of the N-induced level. Upon illumination, carriers are excited from the N-induced level to the conduction-band edge (CBE), leading to an enhanced conductivity. Carrier photoexcitation leads to a rearrangement of the N molecular bonds, with the energy of the photoexcited state of the N-induced level above the CBE. In order for the photoconductivity to decay to its preillumination value, the ground state of the N-induced level must be restored by overcoming the electron-capture barrier,  $E_c$ .



from a dopant-induced complex to a shallow donor or acceptor level. In GaAsN, since the RTA-induced suppression of  $\sigma_{PPC}^N$  is accompanied by a reduction in  $f_{\text{int}}$ , the N-induced level leading to PPC is likely associated with N interstitials. Furthermore, Fig. 4 shows that  $E_a$  decreases with increasing  $x$ , indicating that the N-induced level energy remains in the band gap and approaches the CBE as  $x$  increases. Thus, the increase in  $\sigma_{PPC}^N$  for  $x > 0.006$ , shown in Fig. 1, is due to an increase in the density of N-induced levels.

We now propose a mechanism for the PPC effect in GaAsN. As shown in Fig. 6, the Si- or Te-induced donor level,  $d$ , remains near the CBE in both the “ground” (left) and “photoexcited” (right) states of GaAsN. On the other hand, the energy of the N-induced level in the ground (photoexcited) state of GaAsN is below (above) the GaAsN CBE.<sup>38</sup> Photoexcitation of carriers from the ground state of the N-induced level to the GaAsN CBE leads to an enhanced conductivity, and also induces modifications to the N molecular bond configuration. The photoexcited state of the N-induced level has a higher energy than its ground state, namely, it is above the CBE. When illumination is terminated, carriers in the photoexcited state of the N-induced level are unable to immediately return to the ground state. With the addition of thermal energy,  $E_c$  is overcome and the ground state configuration of the N-induced level is restored. The N-induced level is once again able to accept carriers, and the conductivity decays to its preillumination value. The molecular bond configurational change may be a bond reorientation or a shift in the molecular center of mass. Similarly, two bistable configurations have been reported for C pairs in Si due to a bond reorientation and rotation of the C pair.<sup>39</sup>

#### IV. SUMMARY

In summary, we have investigated the influence of N environment on the PPC effect in GaAs<sub>1-x</sub>N<sub>x</sub>. For  $x > 0.006$ , significant PPC is observed at cryogenic temperatures with the PPC magnitude increasing with increasing  $x$ , due to an increase in the density of N-induced levels. Since RTA suppresses  $\sigma_{PPC}^N$  and reduces  $f_{\text{int}}$ , the N-induced level is likely associated with N interstitials. PPC in GaAsN is attributed to the photoexcitation of carriers from a N-induced level to the CBE, leading to a modified molecular bond configuration of the N-induced level. With sufficient thermal energy, the original N-induced level configuration is restored, and the N-induced level is able to accept carriers once again. The change in molecular bond configuration is likely a bond reorientation or a shift in the center of mass.

#### ACKNOWLEDGMENTS

We thank Stephan Lany for useful discussions. This work is supported by the National Science Foundation (Grant No. DMR 1006835). YJ and RSG were supported in part by the Center for Solar and Thermal Energy Conversion, an Energy Frontier Research Center funded by the U.S. Department of Energy, Office of Science, Office of Basic Energy Sciences, under Award No. DE-SC0000957. TD was supported by the Science Foundation Ireland. RMJ was supported by the Intel Foundation. The NRA studies were supported by the Center for Integrated Nanotechnologies, jointly operated by Los Alamos and Sandia National Laboratories for the U.S. Department of Energy. We also acknowledge the assistance of the staff at the Lurie Nanofabrication Facility at UM.

\*Corresponding author: rsgold@umich.edu

<sup>1</sup>M. G. Craford, G. E. Stillman, J. A. Rossi, and N. Holonyak, *Phys. Rev. B* **168**, 867 (1968).  
<sup>2</sup>D. V. Lang and R. A. Logan, *Phys. Rev. Lett.* **39**, 635 (1977).  
<sup>3</sup>D. V. Lang, R. A. Logan, and M. Jaros, *Phys. Rev. B* **19**, 1015 (1979).  
<sup>4</sup>J. C. Phillips, *Rep. Prog. Phys.* **59**, 1133 (1996).  
<sup>5</sup>E. F. Schubert and K. Ploog, *Phys. Rev. B* **30**, 7021 (1984).  
<sup>6</sup>D. J. Chadi and K. J. Chang, *Phys. Rev. B* **39**, 10063 (1989).  
<sup>7</sup>S. H. Hsu, Y. K. Su, R. W. Chuang, S. J. Chang, W. C. Chen, and W. R. Chen, *Jpn. J. Appl. Phys., Part 1* **44**, 2454 (2005).  
<sup>8</sup>S. H. Hsu, W. R. Chen, Y. K. Su, R. W. Chuang, S. J. Chang, and W. C. Chen, *J. Cryst. Growth* **290**, 87 (2006).  
<sup>9</sup>J. Z. Li, J. Y. Lin, H. X. Jiang, J. F. Geisz, and S. R. Kurtz, *Appl. Phys. Lett.* **75**, 1899 (1999).  
<sup>10</sup>Y. Jin, Y. He, H. Cheng, R. M. Jock, T. Dannecker, M. Reason, A. M. Mintairov, C. Kurdak, J. L. Merz, and R. S. Goldman, *Appl. Phys. Lett.* **95**, 092109 (2009).  
<sup>11</sup>Y. Jin, R. M. Jock, H. Cheng, Y. He, A. M. Mintairov, Y. Wang, C. Kurdak, J. L. Merz, and R. S. Goldman, *Appl. Phys. Lett.* **95**, 062109 (2009).  
<sup>12</sup>P. R. C. Kent and Alex Zunger, *Phys. Rev. B* **64**, 115208 (2001).  
<sup>13</sup>P. R. C. Kent and Alex Zunger, *Appl. Phys. Lett.* **82**, 559 (2003).  
<sup>14</sup>S. Fahy, A. Lindsay, H. Ouerdane, and E. P. O'Reilly, *Phys. Rev. B* **74**, 035203 (2006).

<sup>15</sup>Yong Zhang, A. Mascarenhas, H. P. Xin, and C. W. Tu, *Phys. Rev. B* **61**, 7479 (2000).  
<sup>16</sup>P. J. Klar, H. Gruning, W. Heimbrodt, J. Koch, F. Hohnsdorf, W. Stolz, P. M. A. Vicente, and J. Camassel, *Appl. Phys. Lett.* **76**, 3439 (2000).  
<sup>17</sup>R. Kudrawiec, M. Latkowska, M. Welna, J. Misiewicz, M. Shafi, R. H. Mari, M. Henini, and W. Walukiewicz, *Appl. Phys. Lett.* **101**, 082109 (2012).  
<sup>18</sup>K. Alberi, B. Fluegel, D. A. Beaton, A. J. Ptak, and A. Mascarenhas, *Phys. Rev. B* **86**, 041201 (2012).  
<sup>19</sup>Clas Persson and Alex Zunger, *Phys. Rev. B* **68**, 035212 (2003).  
<sup>20</sup>L. Ivanova, H. Eisele, M. P. Vaughan, Ph. Ebert, A. Lenz, R. Timm, O. Schumann, L. Geelhaar, M. Dahne, S. Fahy, H. Riechert, and E. P. O'Reilly, *Phys. Rev. B* **82**, 161201 (2010).  
<sup>21</sup>Yong Zhang, A. Mascarenhas, J. F. Geisz, H. P. Xin, and C. W. Tu, *Phys. Rev. B* **63**, 085205 (2001).  
<sup>22</sup>A. Patanè, J. Endicott, J. Ibanez, P. N. Brunkov, L. Eaves, S. B. Healy, A. Lindsay, E. P. O'Reilly, and M. Hopkinson, *Phys. Rev. B* **71**, 195307 (2005).  
<sup>23</sup>A. Grau, T. Passow, and M. Hetterich, *Appl. Phys. Lett.* **89**, 202105 (2006).  
<sup>24</sup>J. D. Perkins, A. Mascarenhas, Yong Zhang, J. F. Geisz, D. J. Friedman, J. M. Olson, and S. R. Kurtz, *Phys. Rev. Lett.* **82**, 3312 (1999).

- <sup>25</sup>X. Liu, M.-E. Pistol, and L. Samuelson, *Phys. Rev. B* **42**, 7504 (1990).
- <sup>26</sup>Xiao Liu, M.-E. Pistol, L. Samuelson, S. Schwetlick, and W. Seifert, *Appl. Phys. Lett.* **56**, 1451 (1990).
- <sup>27</sup>M. Reason, H. A. McKay, W. Ye, S. Hanson, R. S. Goldman, and V. Rotberg, *Appl. Phys. Lett.* **85**, 1692 (2004).
- <sup>28</sup>M. Reason, N. G. Rudawski, H. A. McKay, X. Weng, W. Ye, and R. S. Goldman, *J. Appl. Phys.* **101**, 083520 (2007).
- <sup>29</sup>W. Ye, S. Hanson, M. Reason, X. Weng, and R. S. Goldman, *J. Vac. Sci. Technol. B* **23**, 1736 (2005).
- <sup>30</sup>D. Henning and H. Thomas, *Solid-State Electron.* **25**, 325 (1982).
- <sup>31</sup>D. V. Lang and R. A. Logan, in *Physics of Semiconductors 1978* (Inst. Physics, London, UK, 1979), pp. 433–436.
- <sup>32</sup>H. P. Xin, K. L. Kavanagh, Z. Q. Zhu, and C. W. Tu, *Appl. Phys. Lett.* **74**, 2337 (1999).
- <sup>33</sup>H. P. Xin, K. L. Kavanagh, Z. Q. Zhu, and C. W. Tu, *J. Vac. Sci. Technol. B* **17**, 1649 (1999).
- <sup>34</sup>H. Ikoma, *J. Phys. Soc. Jpn* **28**, 1474 (1970).
- <sup>35</sup>E. F. Schubert, *Doping in III-V Semiconductors* (Cambridge University Press, Cambridge, UK, 1993) pp. 193–207.
- <sup>36</sup>C. M. Wolfe, D. M. Korn, and G. E. Stillman, *Appl. Phys. Lett.* **24**, 78 (1974).
- <sup>37</sup>T. Ahlgren, E. Vainonen-Ahlgren, J. Likonen, W. Li, and M. Pessa, *Appl. Phys. Lett.* **80**, 2314 (2002).
- <sup>38</sup>S. B. Zhang and S.-H. Wei, *Phys. Rev. Lett.* **86**, 1789 (2001).
- <sup>39</sup>L. W. Song, X. D. Zhan, B. W. Benson, and G. D. Watkins, *Phys. Rev. Lett.* **60**, 460 (1988).
- <sup>40</sup>S. G. Spruytte, C. W. Coldren, J. S. Harris, W. Wampler, P. Krispin, K. Ploog, and M. C. Larson, *J. Appl. Phys.* **89**, 4401 (2001).